STRUCTURAL CHARACTERIZATION OF PURE AND DOPED CALCIUM PHOSPHATE BIOCERAMICS PREPARED BY SIMPLE SOLID STATE METHOD

Samina Ahmed†, Md. Humayun Kabir*, Farah Nigar*, Sumaya F. Kabir**, Ahmad I. Mustafa* and Mainul Ahsan **

ABSTRACT

Calcium Phosphate based bioceramic materials, in pure and doped forms have been successfully synthesized from egg shells by using solid-state method for the first time. Considering the diverse role of zinc and fluoride in biological functions, these two ions were chosen to develop the substituted bioceramic materials. Structural characterizations of these developed bioceramics were performed by using FTIR, XRD, SEM and EDS techniques. The results revealed that the fluoride doped apatite was formed in single phase containing hydroxyapatite while pure and Zinc doped apatites contained β-TCP with hydroxyapatite. Experimental results and the crystallographic parameters matched well with the literature values indicating that the present experimental protocol favoured the formation of the desired bioceramics. However, to synthesize the ($Ca_3(PO_4)_2$) based bioceramic materials, such a simple solid-state approach would obviously be very helpful, not only in making the process economically feasible, but also in creating an effective material-recycling technology for waste-management.

Keywords: *Bioceramic, Hydroxyapatite, Synthesis, Egg shell, Solid state method.*

1. INTRODUCTION

Recently, synthetic bioceramic materials biocompatible, bioactive and osteoconductive-are extensively used for medical purposes, e.g. bone tissue engineering, bone substitution, and dentistry fields (Sinha, Misra and Ravishankar, 2008; Kabir, Ahmed, Ahsan and Mustafa, 2012). Among the bioceramic materials, Calcium Phosphate based bioceramics have been used for over 30 years in clinical applications (Desai, 2007). However, it is well-known that human bone is a hybrid composition of inorganic (~70 % apatitic calcium phosphate with a Ca/P ratio 1.66) and organic (~30 % collagen) materials (Ahmed and Ahsan, 2008). The apatitic component termed as Calcium hydroxyapatite [HA, $Ca_{10}(PO_4)_6(OH)_2$)] gets enormous attraction as an implant material for bone substitution (Kamitakahara, Takahashi and Ioku, 2012). Indeed the excellent bioactivity, biocompatibility and osteoconductivity makes the hydroxyapatite (HA) as the principal candidate to be used in the fields of orthopaedics, bone tissue engineering, as well as for dental applications. However, in addition to this HA, (where Ca/P molar ratio is 1.67) two other forms of Calcium phosphate e.g. α-tricalcium phosphate (α-TCP) and β-tricalcium phosphate (β-TCP) are also used as biomaterials. However, wider applications of synthetic HA are somewhat restricted due to its poor thermal stability, undesirable fast dissolution rates *in-vivo* and poor mechanical properties, like low-impact resistance (Webster, Massa-Schlueter, Smith and Slamovich, 2004). On the other hand, higher dissolution rate of β-TCP promotes the formation of continuous interface between Calcium Phosphate ceramics and bone. Hence, this biomaterial also received attention of researchers (Ito, and Ichinose, 2005).

Nowadays, researchers are making efforts to develop doped apatites through the substitution of chemical species found in natural bones. Flexible structure of HA admits several substitutions, which can incorporate cations with different oxidation state, but anions with the same oxidation state as that of $-OH^-$ group. Such incorporations play a significant role in synthesizing HA with enhanced mechanical and physiological stabilities that could be used for restoration of hard tissue, such as bone and teeth (Tang, et al., 2009; Tas, Bhaduri and Jalota, 2007). Recently, due to the diverse role of Zinc (Zn) in biological functions, it has been considered as one of the preferable candidates to develop HA in doped form. The slow release of Zn incorporated into an implant material can accelerate the recovery of a patient by promoting bone formation around the implant (Ming'Ou, et al., 2008). On the other hand, fluoride substituted apatite has attracted much attention due to its extensive performance relating to the stability of apatite and also for its preventive role in dental carries (Kannan and Ferreira, 2006). Although a number of techniques (e.g. wet chemical precipitation method, sol-gel method, hydrothermal synthesis procedure, thermal deposition and solid state reaction method) have already been developed (Balázsi, et al., 2007; Feng, Mu-sen, Yu-peng and Yong-xin, 2005) to synthesize the bioceramic materials in both pure and doped form, but the wet chemical precipitation route scores high as the most popular approach.

Considering the above facts, we have focused on developing Calcium phosphate bioceramics in pure and doped form (Zn and fluoride doped) from egg shell

* Bangladesh Council of Scientific and Industrial Research (BCSIR), Dhaka, Bangladesh. † Email: shanta_samina@yahoo.com
** Department of Applied Chemistry and Chemical Engineering, University of Dhaka, Bangladesh.

through a simple-solid state approach. Such an attempt would obviously be beneficial not only to make the process economically feasible, but utilization of egg shell would also create an effective material-recycling technology for waste-management.

2. MATERIALS AND METHODS

2.1 Synthesis of Pure and Doped Calcium Phosphate Bioceramics

Prior to the synthesis of bioceramic materials, raw egg shells were cleaned, washed and dried at 100°C in an oven. The oven-dried egg shells were then powdered and finally characterized as mentioned previously (Kabir, Ahmed, Ahsan and Mustafa, 2011). Analar grade chemicals (ZnO, $(NH_4)_2HPO_4$ and NaF) obtained from either E. Merck or BDH were used.

Pure and doped bioceramics (apatites) were synthesized through a simple solid-state approach described as follows. In order to synthesize pure apatite, requisite amount of egg shell powder and $(NH_4)_2HPO_4$ were mixed thoroughly maintaining Ca/P ratio at 1.66. The mixture was then ball milled for about 8 hrs. While in case of Zn and fluoride doped apatite, ZnO and NaF were added, respectively, to the egg shell powder before ball milling (the ratio of doping precursor and egg shell powder was 1.10). After the completion of the ball milling operation each of the mixture was calcined at 900°C for 30 minutes. The calcination temperature was raised slowly (3°C / min). The apatites thus formed by this solid-state reaction method were then characterized by FTIR, XRD, SEM and EDS techniques.

2.2 Characterization of Pure and Doped Calcium Phosphate Bioceramics

The presence of the functional groups in the developed apatite samples were investigated through the FTIR analysis. FTIR peaks were recorded by using FTIR- Prestige 21 (SHIMADZU). Samples-to-KBr ratio of 1:100 was used to obtain experimental spectra and the samples were scanned in the mid infrared-wave number range of 4000 cm^{-1} to 400 cm^{-1} with an average of 30 scans. The resolution of the spectrometer was 4 cm^{-1}.

The phase analyses of the raw materials and the synthesized apatites were accomplished using X-ray diffractometer (PANalytical X'Pert PRO XRD PW 3040). The intensity data were collected in 0.02° steps at the scanning range of $2\theta = 5° – 90°$ using CuKα (λ = 1.54178°A) radiation. The phases present in the developed Calcium phosphate based bioceramics were compared and confirmed using standard JCPDS files for hydroxyapatite and β-TCP.

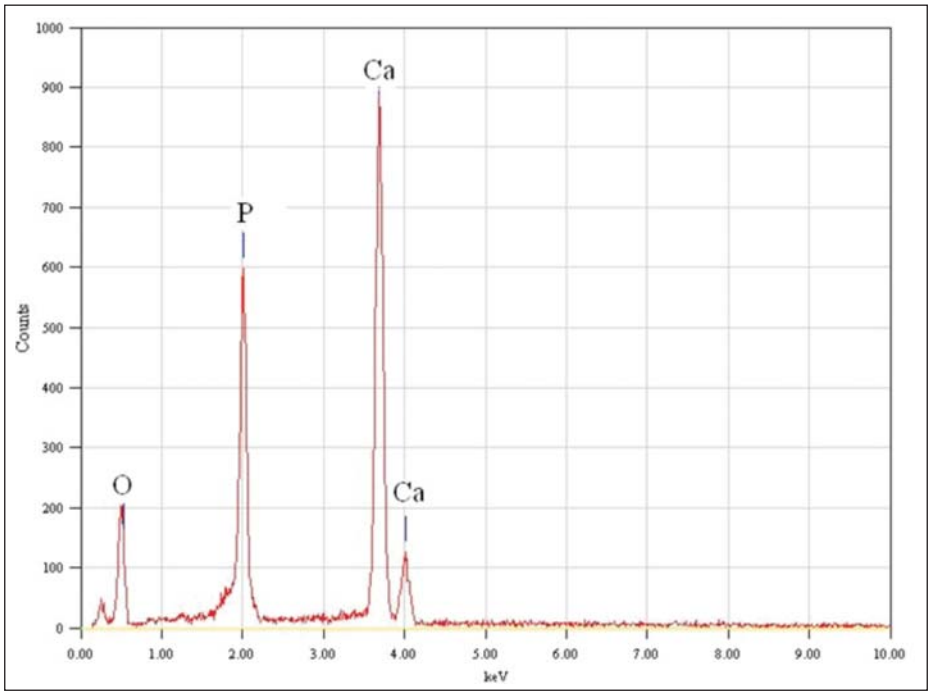

Figure-1(a): EDX Spectrum of Pure Calcium Phosphate Bioceramic

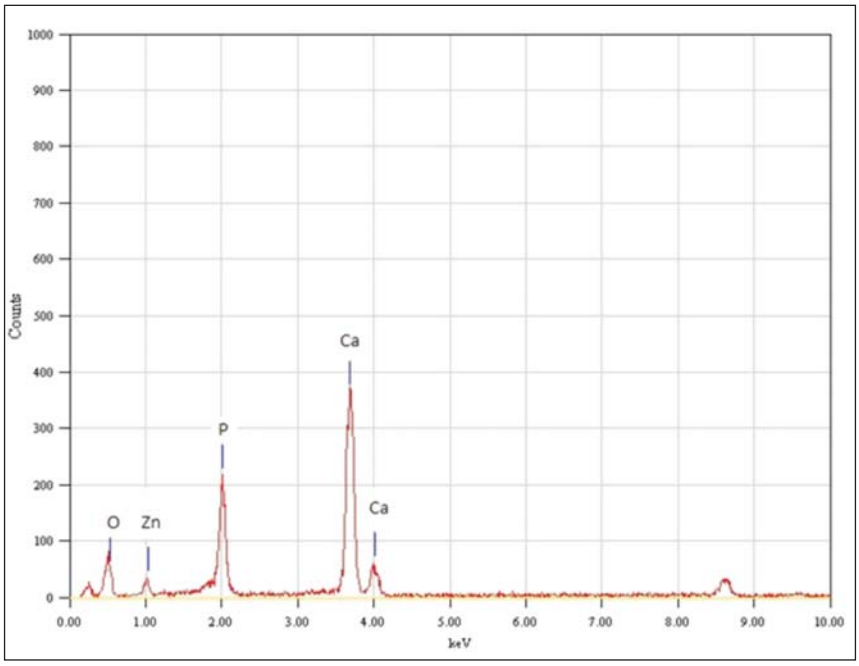

Figure-1(b): EDX Spectrum of Zn Doped Calcium Phosphate Bioceramic

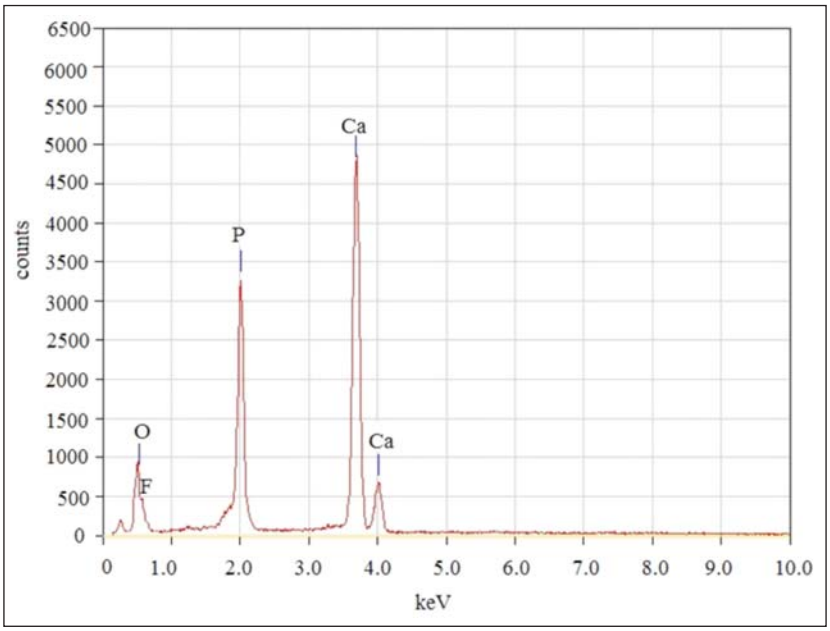

Figure-1(c): EDX Spectrum of F Doped Calcium Phosphate Bioceramic

The surface morphology and microstructural features of the synthesized bioceramic materials were observed by JEOL-JSM 6490LA scanning electron microscope (SEM) equipped with Energy Dispersive X-ray (EDX). The EDX spectra ensured the presence of the expected elements in the synthesized bioceramics.

3. RESULTS AND DISCUSSION

3.1 EDX Analysis

The recorded EDX spectra of the synthesized Calcium Phosphate bioceramic materials are depicted in Figures-1(a – c), which clearly visualize the presence

Table-1: FTIR Band Positions and their Corresponding Assignments

Observed band positions (cm^{-1}) in the Ca-phosphate bioceramics			Corresponding assignments
Pure form	**Zn doped**	**Fluoride doped**	
495.71	445.56	468.70	ν_2 PO_4^{3-} bend
551.64	551.64	570.93	ν_4 PO_4^{3-} bend
607.58	601.79	603.72	ν_4 PO_4^{3-} bend
727.16	--	744.52	CO_3^{2-} group
974.05	--	--	ν_1 PO_4^{3-} stretch
1037.70	1037.70	1047.35	ν_3 PO_4^{3-} stretch
3442.94	3442.94	3441.01	OH^- stretch
--	--	3533.59	OH…F bond

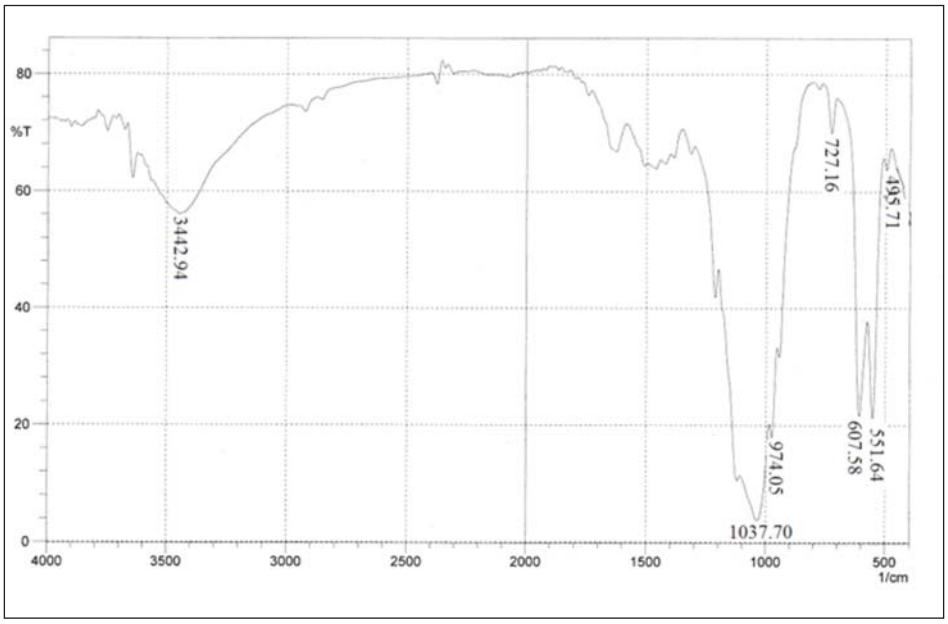

Figure-2(a): FTIR Spectrum of Pure Calcium Phosphate Bioceramic

of the elements Ca, P and O in all the three synthesized samples. However, in addition to these elements, the presence of Zn and F are also evident in the Zn-doped and fluoride doped apatites, respectively (Figures-1(b) and 1(c)).

3.2 FTIR Analysis

The resulted FTIR spectra of the synthesized Calcium phosphate bioceramic materials are shown in Figures 2 (a – c), while the observed band positions and their respective assignments are tabulated in Table-1. It is evident from Table-1 that the corresponding band positions for PO_4^{3-}, CO_3^{2-}, OH^- groups and OH…F bond are well-defined and in excellent agreement with the characteristic FTIR data for crystalline apatite phase as observed in many previous studies (Rameshbabu, Kumar and Rao 2006; Eslami, Solati-Hashjin and

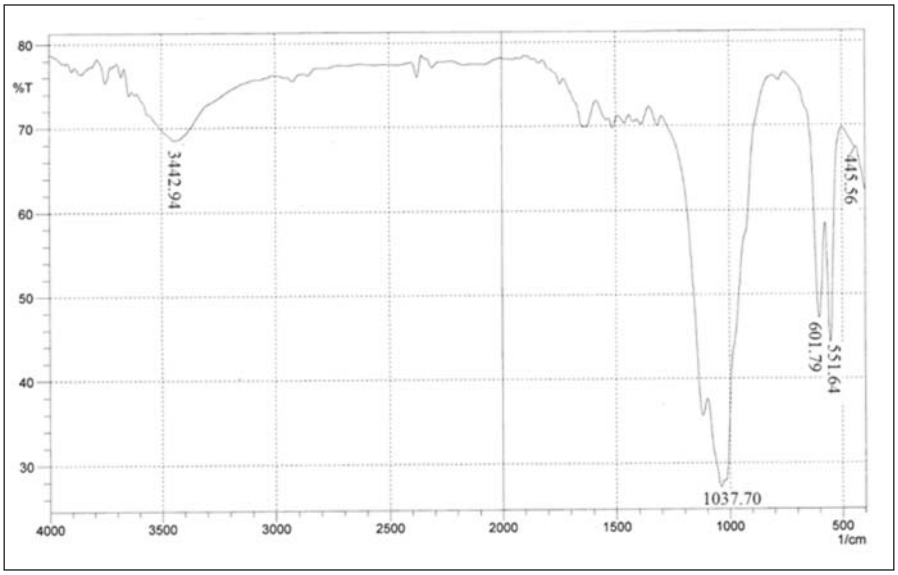

Figure-2(b): FTIR Spectrum of Zinc Doped Calcium Phosphate Bioceramic

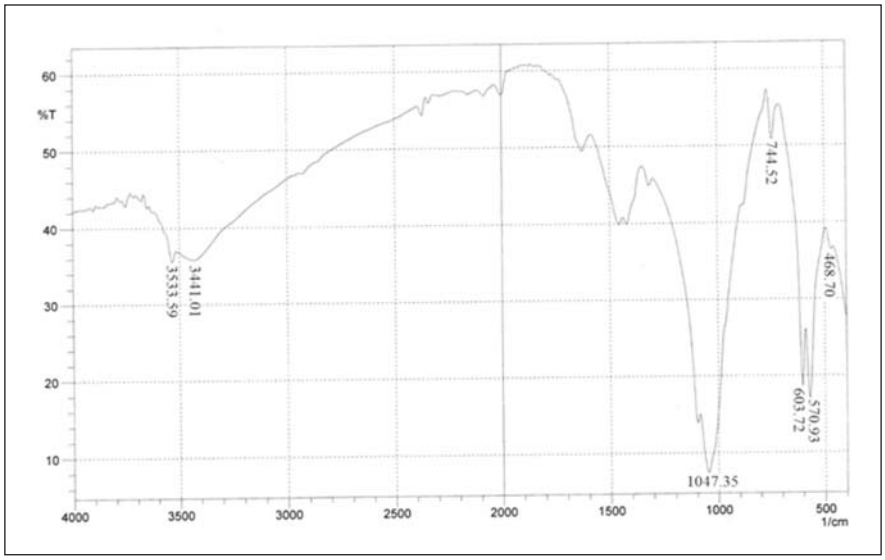

Figure-2(c): FTIR Spectrum of F Doped Calcium Phosphate Bioceramic

Tahriri, 2008; Montazeri, et al., 2010). However, the distinct features of all the synthesized bioceramics are summarized as follows:

i) The noticeable large separation between the two bands at 551.70 cm^{-1} – 570.13 cm^{-1} and 601.79 cm^{-1} – 607.58 cm^{-1} further suggested that the synthesized bioceramic materials are well crystallized and comprised apatitic phase (Ahmed and Ahsan, 2008).

ii) The band positions appeared at 3533.59 cm^{-1} in the fluoride doped apatite represented the stretching mode of OH…F bond. The presence of this band demonstrated that some of the OH^- groups of HA were substituted by F ion as expected.

iii) Another significant observation was the absence of the band at ~632 cm^{-1} in the FTIR spectra of all

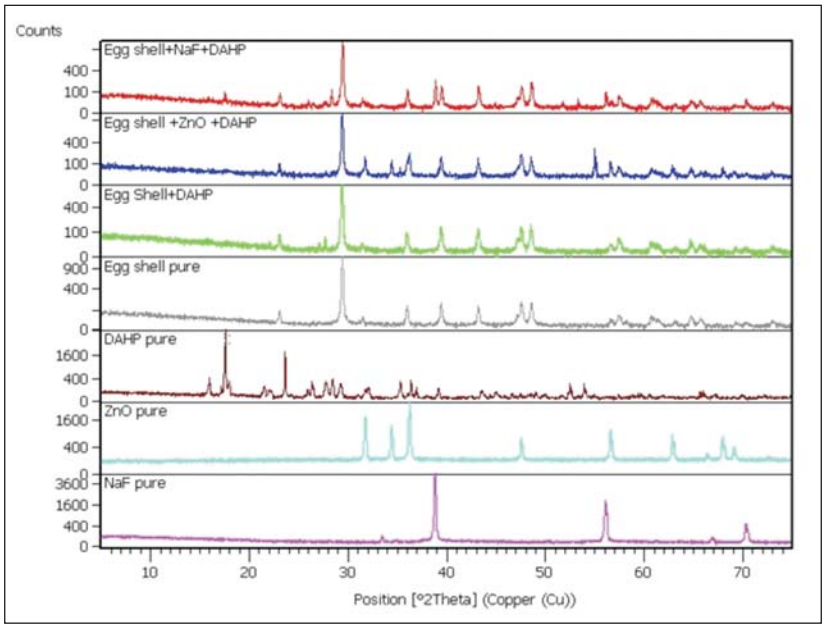

Figure-3: XRD Spectra of the Raw Materials used to Synthesize Pure HA, Zn Doped HA, and Fluoride Doped HA

synthesized samples. The band position at ~632 cm^{-1} signified the presence of structural OH^- (OH liberation mode) in HA (Ahmed and Ahsan, 2008). However, in the case of fluoride doped apatite, lack of this band further ensured the OH^- group of the HA has been substituted by the desired fluoride ion (Montazeri, et al., 2010). On the other hand, in the case of pure and Zn doped apatite, absence of this structural OH^- band at ~632 cm^{-1} indicated the transformation of HA into β-TCP, which is also verified by XRD data.

3.3 XRD Analysis

The XRD spectra of the raw materials (in pure and mixed forms) used for the synthesis of HA and doped apatites are shown in Figure-3. Prior to the XRD, the raw materials were only ball milled but not calcined. Clearly, the XRD spectra of the raw materials (egg shell, ZnO, NaF and di-ammonium hydrogen phosphate, DAHP), show the characteristic peaks for calcite (ICDD Ref. code 01-072-4582), ZnO (ICDD Ref. code 01-070-2551), NaF (ICDD Ref. code 00-001-1181) and DAHP (ICDD Ref. code 00-008-0033), respectively. However, the XRD spectra (Figure-3) of the uncalcined raw materials in mixed form (i. egg shells and DAHP; ii. egg shell, ZnO and DAHP; iii. egg shell, NaF and DAHP) show only the characteristic peaks for the respective raw materials but not for any HA or β-TCP formation. This observation ensured that without sintering no desired product formation occurred.

The XRD spectra of the synthesized bioceramic materials are depicted in Figures-4(a-c). The recorded spectra of pure and Zn doped HA Figures 4(a) and (b) resulted several sharp and intense peaks characteristic of HA and β-TCP. This observation suggests a truly crystalline nature of the synthesized apatites. On the other hand, the XRD of the fluoride doped HA revealed only the peaks of HA. The major d-spacing values as tabulated in Tables 2-3 are compared with the JCPDS standard data for HA (Ref. code:89-6439) and β-TCP (Ref. code:09-0169) (Kannan and Ferreira, 2006; Kannan, Ventura and Ferreira, 2007).

It is obviously confirmed from Tables 2-3 that the fluoride doped apatite is formed in purely single phase containing HA of hexagonal structure (Ahmed and Ahsan, 2008). Particularly, the strong diffraction peaks corresponding for HA at 2θ position 31.87° (2 1 1 plane) together with other two peaks at 32.20° (1 1 2 plane) and 33.03° (3 0 0 plane) of almost equal intensities confirmed the formation of well-crystalline pure HA (Ahmed and Ahsan, 2008). However, the most noteworthy detection was the shift of 2θ positions for (3 0 0), (4 1 0) planes to higher diffraction angles, while (0 0 2), (0 0 4) planes appeared at lower diffraction angles as compared with the JCPDS values

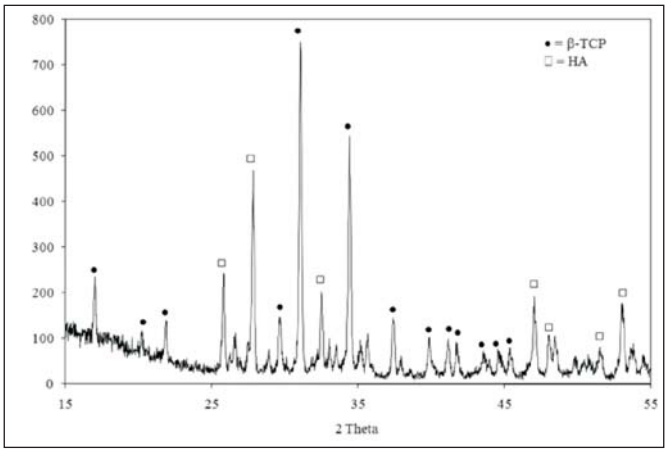

(a)

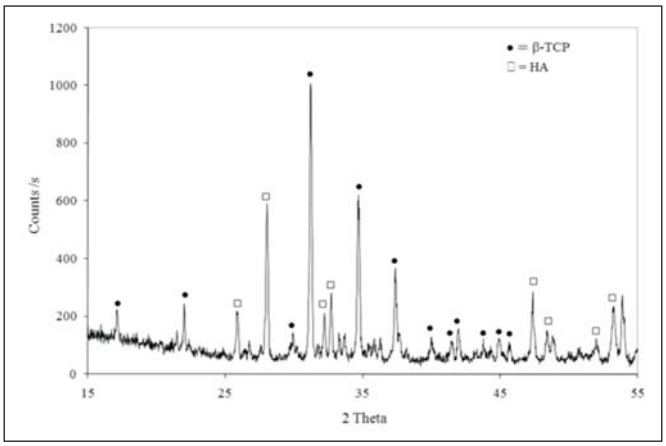

(b)

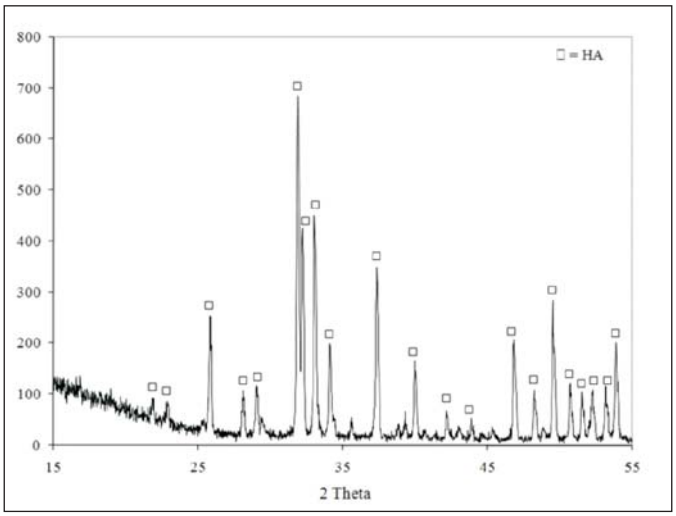

(c)

Figure-4: XRD Spectrum of (a) Pure Calcium Phosphate Bioceramic; (b) Zinc Doped Calcium Phosphate Bioceramic; (c) Doped Calcium Phosphate Bioceramic

Table-2: Comparative d-spacing Values of Synthesized Calcium Phosphate Bioceramics and JCPDS Standards for HA

JCPDS standards for HA		Experimental values of the synthesized Calcium phosphate bioceramics						h k l
		Pure form		Zn doped		Fluoride doped		
d-value	Intensity %	*d*-value	Intensity	*d*-value	Intensity %	*d*-value	Intensity %	
4.077	6.40	4.060	17.14	--	--	4.060	11.84	2 0 0
3.440	35.50	3.450	31.80	3.440	17.76	3.446	36.81	0 0 2
2.813	100.00	2.812	6.60	2.812	5.45	2.810	100.00	2 1 1
2.774	47.60	2.779	6.52	2.777	15.47	2.778	61.12	1 1 2
2.718	64.20	2.710	9.19	--	--	2.710	67.12	3 0 0
2.629	21.90	--	--	--	--	2.629	23.90	2 0 2
2.261	22.20	2.260	12.64	2.253	7.95	2.255	20.49	1 3 0
1.943	27.60	1.932	19.76	1.948	1.82	1.940	28.18	2 2 2
1.840	30.30	--	--	--	--	1.840	41.00	2 1 3
1.720	13.70	1.721	15.77	1.720	18.59	1.722	15.77	0 0 4

Table-3: Comparative d-spacing Values of Synthesized Calcium Phosphate Bioceramics and JCPDS Standards for β-TCP

JCPDS standards for β-TCP		Experimental values of the synthesized Ca-phosphate bioceramics				h k l
		Pure form		Zn doped		
d-value	Intensity %	*d*-value	Intensity %	*d*-value	Intensity %	
3.00	12.20	3.01	17.85	2.99	10.39	3 0 0
2.87	100.00	2.87	100.00	2.86	100.00	0 2 10
2.75	22.20	2.75	26.21	2.74	24.55	1 2 8
2.61	64.80	2.61	60.97	2.59	58.48	2 2 0
2.07	5.50	2.07	7.03	2.07	7.54	0 0 18

Table-4: Calculated Crystallographic Parameters for the Synthesized Calcium Phosphate Bioceramics

Ca-phosphate bioceramics	Identified phases	Calculated crystallographic parameters	JCPDS data
Pure form	β-TCP (dominant phase)	*a* = 10.44 Å, *c* = 37.37 Å *V* = 3527.29 Å	(for β-TCP) *a* = 10.43 Å *c* = 37.38 Å *V* = 3520.91 Å (for HA) *a* = 9.41 Å *c* = 6.88 Å *V* = 1577.25 Å (for F-HA) *a* = 9.37 °A *c* = 6.88 °A *V* = 1563.2 Å
	HA	*a* = 9.42 Å, *c* = 6.88 Å *V* = 1580.6 Å	
Zn doped	β-TCP (dominant phase)	*a* = 10.39 Å, *c* = 37.26 Å *V* = 3483.3 Å	
	HA	*a* = 9.39 Å, *c* = 6.86 Å *V* = 1565.98 Å	
Fluoride doped	Fluoroapatite (F-HA) (single phase)	*a* = 9.37 Å, *c* = 6.89 Å *V* = 1566.1 Å	

for pure HA. This observation is quite consistent with the previous results (Barinov, et al., 2004). These shifts indicated the substitution of OH^- with F ions in the apatite structure (Montazeri, et al., 2010) and are characteristic of fluoride doped hydroxyapatite formation. Such observation obviously validated the FTIR spectral data, as illustrated previously.

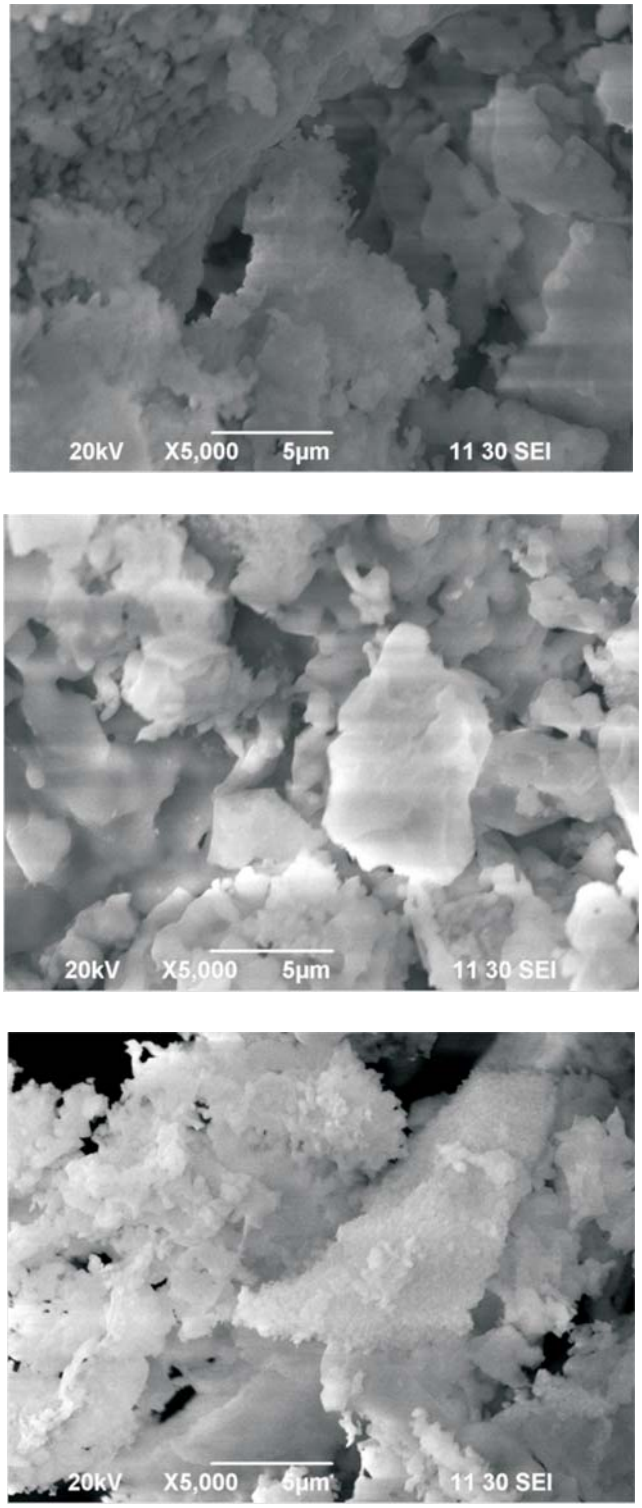

(a)

(b)

(c)

Figure-5: XRD Spectrum of (a) Pure Calcium Phosphate Bioceramic; (b) Zn Doped Calcium Phosphate Bioceramic; (c) F Doped Calcium Phosphate Bioceramic

On the other hand, in the case of pure and Zn doped apatites although the presence of HA phase was visible (Table-2), but β-TCP of rhombohedral structure was indexed as the dominating phase (Table-3). Particularly the corresponding diffraction peaks for (3 0 0), (0 2 10) and (2 2 0) planes reflected the presence of β-TCP along with the HA. The volume fraction (X_β) of β-TCP was estimated using the following equation (Saranya, Kowshik and Ramanan, 2011).

$$X_\beta = \frac{PW_\beta}{[1+(P-1)W_\beta]} \quad \text{.....(1)}$$

$$\text{where } W_\beta = \frac{I_\beta}{I_\beta + I_{HA}} \quad \text{.....(2)}$$

I_β and I_{HA} are the XRD intensity values of β-TCP at [0 2 10] and HA at [2 1 1] reflections, respectively. The coefficient P is the integrated intensity ratio of HA at [2 1 1] to β-TCP at [0 2 10] reflection. The value of P was determined as 2.275 using the XRD of the mixtures of standard HA and β-TCP (Saranya, Kowshik and Ramanan, 2011). Percent (%) volume fraction (X_β) of β-TCP in synthesized pure and Zn doped HA was found to be 97 and 98, respectively. Thus, calcination of HA at 900°C facilitated the formation of β-TCP according to the following equation:

$$Ca_{10}(PO_4)_6(OH)_2 \rightarrow 3\,Ca_3(PO_4)_2 + CaO + H_2O \quad \text{.....(3)}$$

3.4 Crystallographic Parameters

The crystallographic parameters of the synthesized pure and doped (Zn and F doped) bioceramics (both hydroxyapatite and β-TCP) were calculated using the Equation-4, which is usually used for both hexagonal and rhombohedral crystal systems, because rhombohedral crystal system belongs to the special type of trigonal class and the difference between the trigonal and hexagonal system is the symmetry. A hexagonal unit cell has C_6 symmetry, whereas a trigonal unit cell has C_3 symmetry.

$$\frac{1}{d^2} = \frac{4}{3}\left(\frac{h^2+hk+k^2}{a^2}\right) + \frac{l^2}{c^2} \quad \text{.....(4)}$$

The volume (V) of the hexagonal unit cell for HA and the rhombohedral unit cell for β-TCP were calculated using Equations 5 and 6, respectively.

$$V = 2.589a^2c \quad \text{.....(5)}$$

and $$V = 0.866a^2c \quad \text{.....(6)}$$

Given in Table-4 are the calculated crystallographic parameters for all the samples as compared with the standard JCPDS files (Kannan, Ventura, Ferreira, 2007; Barinov, et al., 2004). The experimental values of pure and F doped form of Calcium phosphate bioceramics are in good agreement with the standard JCPDS data. The contraction of a-axis of the fluoride doped apatite (Table-4) is because of the smaller size of F ion (ionic radius = 1.36) compared to -OH ion (ionic radius = 1.68). On the other hand, the values of a and c-axes of Zn doped bioceramic are slightly smaller than the JCPDS values. Such contraction in a and c-axes reflects the effect of smaller ionic radius of Zn^{+2} (0.74) than the Ca^{+2} (0.99) (Miyaji, Kono and Suyama, 2005).

3.5 SEM Observation

The recorded SEM images (5000 magnification) of the three types of synthesized apatites are shown in Figures 5(a-c). All of these SEM micrographs visualized an aggregate consisting of interconnected particles. However, the grain sizes of the synthesized apatites were in the following order: Zn doped apatite > pure apatite > F.e doped apatite.

4. CONCLUSIONS

Considering the importance of bioceramic materials in the fields of orthopaedics and dentistry, Calcium phosphate based bioceramics in pure and doped form (Zn and fluoride doped) have been successfully synthesized from egg shell by solid state method for the first time. Under the present experimental protocol, pure and Zn doped bioceramics were formed in mixed phases where β-TCP was the dominant phase along with small amount of the HA phase. On the other hand, fluoride doped apatite was synthesized in single phase, which was solely fluoroapatite (F-HA). Experimental results were validated using the JCPDS standard values, and a very promising matching between the experimental data and the JCPDS values was observed.

Since choices of raw materials and the methodology are very important in developing a cost-effective protocol, egg shell was chosen as the raw material of

Ca source, while simple solid-state reaction was followed to synthesize the Calcium phosphate based bioceramic materials. Thus, such selection would obviously be very helpful not only to make the process economically feasible, but also to create an effective material-recycling technology for waste-management.

5. ACKNOWLEDGEMENTS

The authors appreciate the financial support of BCSIR to carry out this research work. The generous help provided by the Centre for Advanced Research for Science (CARS), University of Dhaka, to accomplish the SEM/EDS analyses is also thankfully acknowledged.

REFERENCES

- Ahmed, S., and Ahsan, M., 2008. Synthesis of Ca-hydroxyapatite bioceramic from egg shell and its characterization. *Bangladesh Journal of Scientific and Industrial Research*, 43(4), pp.497-508.
- Balázsi, C., et al., 2007. Preparation of calcium–phosphate bioceramics from natural resources. *Journal of the European Ceramic Society*, 27(2-3), pp.1601-1609.
- Barinov, S.M., et al., 2004. Solid solution formation at the sintering of hydroxyapatite–fluorapatite ceramics. *Science and Technology of Advanced Materials*, 5(5-6), pp.537-541.
- Desai, A.Y., 2007. Fabrication and Characterization of Titanium-doped Hydroxyapatite Thin Films, M. Phil. University of Cambridge.
- Eslami, H., Solati-Hashjin, M., and Tahriri, M., 2008. Synthesis and characterization of nanocrystalline fluorinated hydroxyapatite powder by a modified wet-chemical process. *Journal of Ceramic Processing Research,* 9(3), pp.224-229.
- Feng, W., Mu-sen, L., Yu-peng, L., and Yong-xin, Q., 2005. A simple sol–gel technique for preparing hydroxyapatite nanopowders. *Materials Letters,* 59(8-9), pp.916-919.
- Ito, A., and Ichinose, N., 2005. Zinc-containing tricalcium phosphate and related materials for promoting bone formation. *Current Applied Physics,* 5, pp.402-406.
- Kabir, S.F., Ahmed, S., Ahsan, M., and Mustafa, A.I., 2011. Doped hydroxyapatite from waste calcium source: Part 1 – Na doped apatite, *Material Science: An Indian Journal,* 7(1), pp.42-48.
- Kabir, S.F., Ahmed, S., Ahsan, M., and Mustafa, A.I., 2012. Investigation of Sintering Temperature and Concentration effects on sodium doped Hydroxyapatite. *Trends in Biomaterials and Artificial Organs,* 26(2), pp.56-63.
- Kamitakahara, M., Takahashi, H., and Ioku, K., 2012. Tubular hydroxyapatite formation through a hydrothermal process from β-tricalcium phosphate with anatase. *Journal of Materials Science,* 47, pp.4194-4199.
- Kannan, S., and Ferreira, J.M.F., 2006. Synthesis and thermal stability of hydroxyapatite-β-tricalcium phosphate composites with co-substituted sodium, magnesium, and fluorine. *Chemistry of Materials*, 18, pp.198-203.
- Kannan, S., Ventura, J.M., and Ferreira, J. M. F., 2007. Aqueous precipitation method for the formation of Mg-stabilized-β-tricalcium phosphate: An X-ray diffraction study. *Ceramics International,* 33(4), pp.637-641.
- Ming'Ou, L., et al., 2008. Structural characterization of zinc-substituted hydroxyapatite prepared by hydrothermal method, *Journal of Materials Science: Materials in Medicine*, 19, pp.797-803.
- Miyaji, F., Kono, Y., and Suyama, Y., 2005. Formation and structure of zinc-substituted calcium hydroxyapatite, *Materials Reserach Bulletin,* 40, pp.209-220.
- Montazeri, L., et al., 2010. Hydrothermal synthesis and characterization of hydroxyapatite and fluorhydroxyapatite nano-size powders, *Biomedical Materials*, doi:10.1088/1748-6041/5/4/045004.
- Rameshbabu, N., Kumar, T.S.S., and Rao, K.P., 2006. Synthesis of nanocrystalline fluorinated hydroxyapatite by microwave processing and its in vitro dissolution study. *Bulletin of Materials Science*, 29(6), pp.611-615.
- Saranya, K., Kowshik, M., and Ramanan, S.R., 2011. Synthesis of hydroxyapatite nanopowders by sol-gel emulsion technique, *Bulletin of Materials Science,* 34(7), pp.1749-1753.
- Sinha, A., Misra, T., and Ravishankar, N., 2008. Polymer assisted hydroxyapatite microspheres suitable for biomedical application. *Journal of Materials Science: Materials in Medicine,* 19, pp.2009-2013.
- Tang, Y., et al., 2009. Zinc incorporation into hydroxylapatite. *Biomaterials,* 30, pp.2864-2872.
- Tas, A.C., Bhaduri, S.B. and Jalota, S., 2007. Preparation of Zn-doped β-tricalcium phosphate (β-$Ca_3(PO_4)_2$) *bioceramics. Materials Science and Engineering C: Materials for Biological*

Applications, 27(3), pp.394-401.

- Webster, T.J., Massa-Schlueter, E.A., Smith, J.L., and Slamovich, E.B., 2004. Osteoblast response to hydroxyapatite doped with divalent and trivalent cations. *Biomaterials,* 25(11), pp.2111-2121.